REVIEW ARTICLE

Strategies toward improving the performance of organic electrodes in rechargeable lithium (sodium) battery

Received 00th January 20xx,
Accepted 00th January 20xx

Yugen Zhang,* Jinquan Wang and Siti Nurhanna Riduan

This article focuses on recent developments on new strategies and approaches of improving the performance of organic electrodes for rechargeable lithium (sodium) battery. It is specifically focus on organic electron acceptor materials, and prospective of the field.

1. Introduction

Since first being commercialized in 1991 by Sony, lithium ion battery (LIB) has dominated the market as the energy storage device of choice for portable electronics.[1-4] Recently, efforts have been devoted to develop energy storage technologies for systems requiring large amounts of power, such as electric vehicles and energy storage stations.[5-6] While rechargeable lithium (sodium) batteries are very attractive candidates, current technologies of inorganic (metal oxides and phosphates) cathode materials face challenge in improving energy densities.[7-9] Organic electrode materials were conceived as early as their inorganic counterparts;[10] however, the progress of development of organic electrode materials for rechargeable battery applications remains stagnant.[11-13] Due to the advantages of low cost and sustainability of naturally abundant elements, environmental benignity, high capacity, excellent structural versatility and flexibility, there has been a resurgence of interest in organic electrode materials.[14-16] Various types of organic materials, including traditional conducting polymers,[17-21] organic radical compounds,[22-26] organodisulfides,[27-31] carbonyl compounds[32-35] and carbon/nitrogen compounds,[36-41] have been investigated as electrode materials. Despite the abovementioned advantages, their low redox stability, high solubility in electrolyte and low electronic conductivity are crucial limitations. Most of organic electrode materials cannot reach their full theoretical capacity. Some organic compounds suffer from rapid capacity decay during cycling, low discharge potentials and others require a large amount of conductive carbon as an additive. Overcoming such intrinsic drawbacks will lead to successful application of such organic electrode materials for rechargeable batteries.[42-52] Although there have been several recent review papers covering the topic,[11,13,36, 54-61] this article focuses on recent developments on improving the performance of organic electrodes for rechargeable lithium (sodium) battery. There are several important parameters in determining the performance of a solid-state battery electrode: (1) redox potential, (2) redox stability and cycling stability, (3) reaction rate of the redox site, (4) solid-state ion transport, and (5) electronic conduction. Various strategies have been applied towards improving of these parameters. This article addresses recent progress on organic electron acceptor materials, and aims to provide a perspective of the field rather than a comprehensive literature review. Scheme 1 listed structures and abbreviations of all related redox active molecules. Table 1 summarized electrochemical performance of all organic electrode materials described in this article.

2. Structure –dependent electrochemical properties of redox active organic compounds

The core of the redox active compounds that can be used as organic electrode materials often consists of reversible redox active chemical bonds, such as C=O and C=N bonds (Scheme 2) with chemical structures surrounding or supporting the redox active bonds deciding the overall performance of the organic electrode materials.[11,13] While there are limited types of redox active bonds of suitable potential to be used as electrode material, there are almost infinite possibilities to improve their performance by modifying the surrounding structures.

As the electrochemically reduced carbonyl group possesses a negative charge, it is important to have certain functional structure to stabilize the molecule. Chen's group[38] systematically analyzed various carbonyl electrodes, and combined experimental and computational studies to propose a rule to predict the design of multi-carbonyl molecular electrodes in multi-electron reactions. When a carbonyl is reduced, the resultant negative charge will be delocalized with the formation of an enol. Delocalization of the negative charge over an extended conjugated aromatic structures and the presence of adjacent carbonyl moieties would further stabilize the final structure.[62,63] The highest occupied molecular orbital (HOMO) plot provides qualitative information on the electronic

Institute of Bioengineering and Nanotechnology, 31 Biopolis Way, The Nanos, Singapore 138669 (Singapore), Email: ygzhang@ibn.a-star.edu.sg.

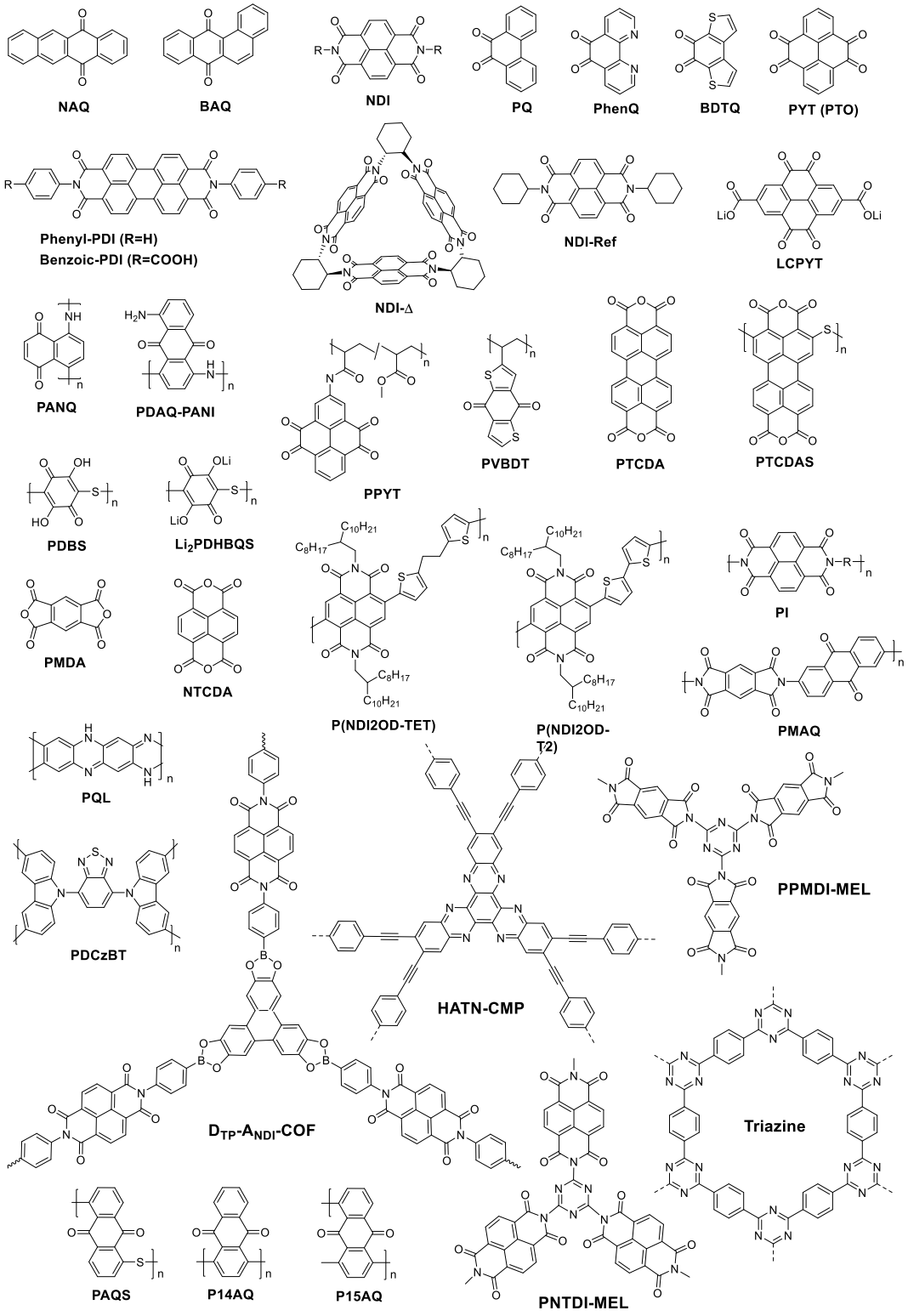

Scheme 1 Redox active molecules: structures and abbreviations.

structure which could potentially predict the carbonyl utilization rate. This is an important strategy for designing new molecules that will allow us to fully utilize their redox active functionalities. Introduction of additional electron-withdrawing groups would lead to higher redox potential of organic molecules,[62] with the lowest unoccupied molecular orbital (LUMO) generally correlating to the reduction potential of organic electrodes.[64] By embedding pre-aromatic 1,2-

dicarbonyls into extended conjugated structures, the reduction potential could be adjusted (Scheme 3). Cho et al studied the isomeric effect between 5,12-naphthacenequinone (NAQ) and 1,2-benzanthraquinone (BAQ).[65] BAQ has lower LUMO energy, which contributes to its higher potential, and possesses a smaller energy gap (between LUMO and HOMO), leading to better conductivity and its better electrochemical performance including higher stability and rate capacity. A similar study has also been demonstrated on naphthalene diimide (NDI) based materials.[66] The reduction potential could varied from 2.3 to 2.9 V vs Li/Li+ with different substitutions (NMe_2, electron donating group; and CN, electron withdrawing group) on NDI.

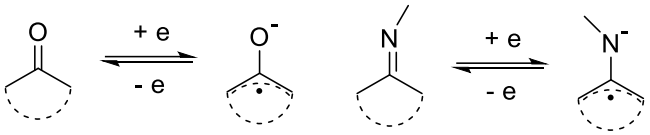

Scheme 2 Electrochemically active bonds with negative charge delocalization structures.

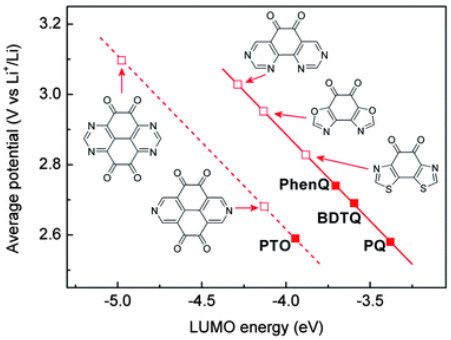

Scheme 3 Correlation between the average working potentials and calculated LUMO energies of phenanthraquinone (PQ), benzo[1,2-b:4,3-b']dithiophen-4,5-quinone (BDTQ), and 1,10-phenanthroline-5,6-dione (PhenQ) (solid dots), exhibiting linear dependence. Following this track, molecules with even more negative LUMO energies and hence higher potentials are proposed (open dots)[38].

Computational modeling is a useful tool in the structural design of such organic cathode materials. Density function theory **(**DFT) computational studies propose that the reduction potential of conjugated carbonyl molecules can be calculated using free energy difference of the reaction ΔG, and the calculated potentials correlated well to experimental data.[67] Furthermore, an index denoted as ΔC2Li was introduced based on Clar's theory[68] to characterize the aromaticity change during lithiation of polycyclic aromatic hydrocarbons (Scheme 4).[69] ΔC2Li is defined as ΔC/0.5ΔLi, where ΔC and ΔLi are the changes in the number of Clar sextets and adsorbed lithium atoms during lithiation. A positive ΔC2Li indicates the aromaticity increase after lithiation and consequently means higher voltage. Based on this theory, one can design high-voltage carbonyl cathode materials; however, the actual organic synthesis may be a challenge.

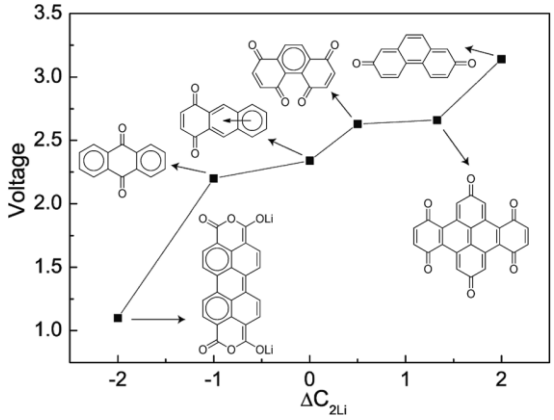

Scheme 4 Voltage variation with ΔC2Li.[69]

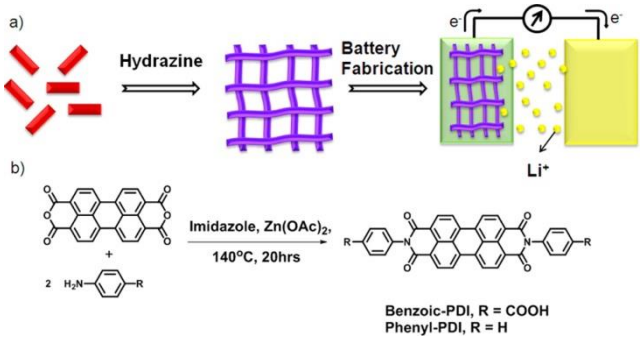

Scheme 5 (a) Cartoon showing the lithium-battery fabrication procedure using reduced benzoic-PDI. The red rod is PDI monomers and the pruple network is reduced PDI. (b) Synthesis of benzoic-PDI and phenyl-PDI.[70]

Recently, a simple chemical reduction approach strategy was developed for modifying redox active molecule and improving the electrochemical performance in LIB application (Scheme 5).[70] The reduction of benzoic-PDI or phenyl-PDI (perylene diimide) by hydrazine leads to dramatically improved electrochemical performances. The specific capacity for reduced benzoic-PDI was reported to be 85 and 107 mAh g^{-1} at 1 C and 10 C respectively, in contrast to 60 and 30 mAh g^{-1} at 1 C and 10 C for untreated benzoic-PDI. The battery equipped with reduced benzoic-PDI cathode exhibits 100% Coulombic efficiency, increased specific capacity at discharging at 20 C and very good stability. Although the detailed mechanism of this approach is not clear, the experimental results are very prove to be very attractive.

3. Strategies toward reducing solubility of organic compounds in electrolytes

A critical limitation of organic electrode materials includes its high solubility in battery electrolyte media, leading to diminished stability in the charge-discharge cycle and a shorter battery life. Various strategies have been proposed to overcome this, and recent examples are presented and analysed here.[34-59] Although solubility of the electrode could also be minimized utlizing a solid electrolyte,[70] this section will

focus on strategies of modifying the electrode materials themselves.

3.1 Oligomerization and salt formation of small molecules

A simple strategy of reducing solubility of organic molecule is to enlarge the backbone structure; however, this will increase its molecular weight and sacrifice the specific capacity when it is used as electrode material. Oligomerization of small molecules would be an efficient method to enlarge the molecular structure while not necessarily increasing molecular weight per functional unit. One excellent example which demonstrated this strategy includes a recent report on a rigid naphthalenediimide (NDI) trimer.[72] It forms a rigid shape-persistent triangle (NDI-Δ) which will decrease the solubility of NDI during redox cycling. Interestingly, it was revealed experimentally and computationally that the electrochemical reaction could be stabilized through space electron delocalization across the overlapping π-orbitals of the three NDI units in the triangular conformation.[73] Furthermore, the rigid structure introduces an intrinsic nanoporosity that may be beneficial to lithium diffusion. This simple strategy improves several aspects of organic cathode materials including stability (lower solubility) and rate capacity (nanoporosity for lithium diffusion and overlapping π -orbitals for electron conductivity). In fact, when used as a cathode material in rechargeable LIB, NDI-Δ demonstrated remarkable improved performance as compared to NDI monomer (Scheme 6). A capacity of 146.4 mAh g^{-1} (theoretical capacity 154.8 mAh g^{-1}) at low current rate of 0.1 C and a capacity of 58.1 mAh g^{-1} at an ultrahigh rate of 100 C were achieved. In contrast, a capacity of less than 10 mAh g^{-1} at 1 C current rate was observed for monomeric NDI. In addition, the battery with NDI-Δ cathode maintains a capacity of 71.1 mAh g^{-1} after cycling at 10 C for 300 cycles.

Forming salts of small organic compounds could reduce their solubility via increasing their polarities,[44-47] and this principle has been demonstrated in many examples, especially in multi-carbonyl redox active compounds. Recently, a report on an interesting approach to enhance cyclability of lithium battery by introducing lithiooxycarbonyl groups onto organic cathode materials was published.[74] Lithium batteries using *p*- and *o*-quinones with two $–CO_2Li$ groups as cathode materials demonstrated much better cycling stability as compared to their parent quinones. Taking LCPYT (pyrene-4,5,9,10-tetraone with two lithiooxycarbonyl groups) as example, the resultant battery exhibits very good capacity (257 mAh g^{-1}, 87% of theoretical capacity, at 1 C), good stability (200 mAh g^{-1} after 100 cycle at 0.2 C) and good rate capacity (192 mAh g^{-1} at 5 C). It is proposed that the lithium carboxylate groups of quinones coordinate together to a form polymeric network which very efficiently reduces the solubility of substituted quinones (Scheme 7). In addition, good electrochemical performance of LCPYT may also due to the ordered network structure which improves the interlayer electronic conductivity via efficient π - π stacking.[75,76] The effect of the ordered arrangement of the carboxylate salts in improving the electrochemical performance was also observed in other systems..[77]

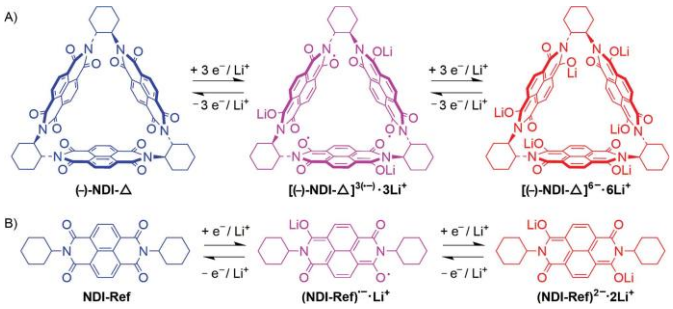

Scheme 6 Structural formulas and redox processes for NDI-Δ and NDI-Ref.[72]

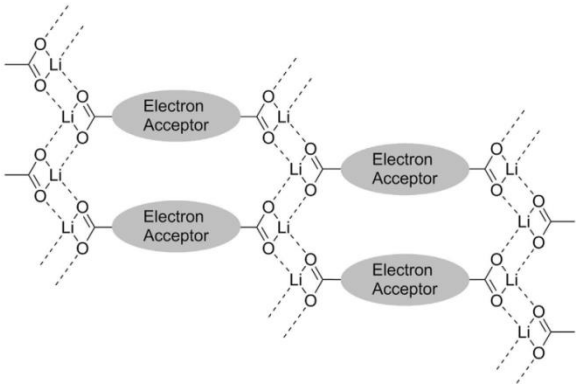

Scheme 7 Schematic drawing of the role of R-CO_2Li groups.[74]

3.2 Polymeric organic electrode materials

Polymerization of organic electrode material is a simple and widely used method to improve the cycling stability of battery.[34-35, 42-44] This section will focus on recent development of polymeric organic electrode materials which adds further improvements other than stability.

3.2.1 Organic compounds with conductive polymer backbones

Cathodes fabricated from most traditional conductive polymers (such as polyaniline (PAN)) intrinsically suffer from their less than ideal capacity utilization and poor cycling stability, mainly due to the low doping degrees and dissolution issue.[11-13, 55] One strategy of overcoming this drawback is to conjugate an electron-acceptor redox active unit onto the conductive polymer chain.[34] This design will change cathodic reaction mechanism of p-type polymers from doping/dedoping processes to the insertion/extraction reactions of Li^+ cation. Additionally, redox active units that sit on backbone of a p-type polymer can serve as electron highway even at low doping level. This design could improve both solubility and conductivity issues of small redox active compounds by binding them onto a polymer chain. One recent example is of poly(1,5-diaminoanthraquinone) (PDAQ-PANI).[78] This organic cathode material includes benzoquinone conjugated onto conducting polyaniline backbone, where the cathodic reaction of this polymer predominantly involves Li^+ insertion/extraction processes. It can deliver a rather high specific capacity of 285 mAh g^{-1} at 20 mA g^{-1}, good rate capacity with 125 mAh g^{-1} at 800

mA g-1 and good stability with capacity retention of 160 mAh g^{-1} over 200 cycles.

3.2.2 Redox active molecules bound on flexible polymer chain

Improved solubility issues and cycling stabilities have also been reported for non-conjugated polymers with redox active moieties.[43, 79-83] Interestingly, examples of organic cathode materials with planar electron acceptor molecules bound precisely onto a flexible backbone with short and constant intervals, exhibit excellent rate capacity. This phenomenon may be due to the electron hopping between the well-organized redox active moieties, which enhance the electronic conductivity of the cathode materials (Scheme 8). Yoshida *et al.*[84] reported a polymer-bound pyrene-4,5,9,10-tetraone (PPYT) as cathode material that exhibits excellent charge-discharge properties with a high specific capacity of 231 mAh g^{-1}, cycling stability (83% of the capacity retained after 500 cycles at 1C), and rate capacity (90% of the capacity at 30 C as compared to 1 C). In contrast, less than 50% of the capacity was retained for the PYT monomer after only 20 cycles at 0.2 C. In this material, PYT units were grafted onto the polymethylacrylate and the π - π stacking/crystalizing may occur within certain range (Scheme 9). In another example, vinyl dithiophenedione was synthesized and polymerized resulting in a polyethylene polymer with dithiophenedione grafted at very short intervals (PVBDT).[85] When used as cathode, the polymer exhibits a capacity of 217 mAh g^{-1} (100% of theoretical capacity) with only 10 wt% of conductive materials and exhibit excellent rate capacity with negligible capacity loss at 10 C as compared to 1 C. However, the cycling stability of this cathode material was not optimal (52% of capacity retained after 100 cycles), and could be due to the poor redox stability of the dithiophenedione unit.

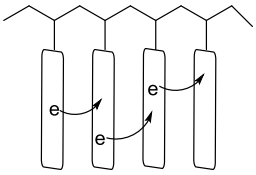

Scheme 8 Electron hopping between the well-organized redox active molecules.

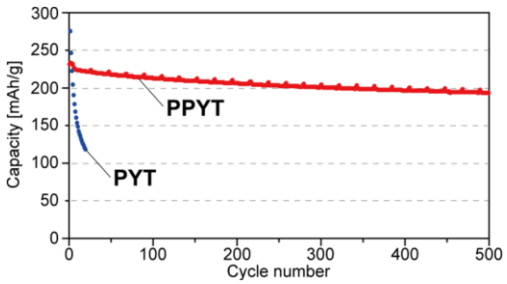

Scheme 9 Extended charge–discharge cycling of PPYT and PYT. PPYT (red dots, 500 cycles, 1 C rate), PYT (blue dots, 20 cycles, 0.2 C rate).[84]

3.2.3 Sulfur bridged redox active compounds as organic cathode materials

Another strategy in preventing the dissolution of organic moieties when used as electrodes includes utilizing sulfur to bridge aromatic backbones of redox active moieties, forming sulfide polymers.[86,87] Additionally, thioether bonds of the polymer could enhance electron transfer between aromatic rings via the lone pair of electrons on sulfur, improving the electronic conductivity when used as a cathode material.[88]

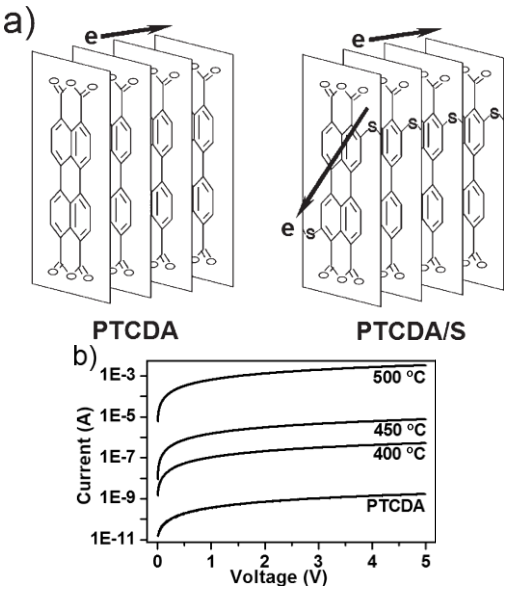

Scheme 10 The electronic conductivity for PTCDA and the sulfide polymers. a) Schematic diagram showing the contribution of thioether bonds to the electronic conductivity. The arrows represent the interlayer or intralayer electron transfer between PTCDAs, respectively. b) I–V curves measured by the linear scanning voltammetry. The polymer samples synthesized at different temperature show much higher conductivity than PTCDA, which increases remarkably with increasing sulfur content, verifying the analysis in (a).[89]

Sun et al. reported a sulfide polymer of 3,4,9,10-perlenetetracarboxylic acid dianhydride (PTCDA) (Scheme 10),[89] where the resistance of sulfide polymer was six orders lower than PTCDA monomer (1.5×10^3 Ω *vs* 4.6×10^9 Ω). As a result, the polymer exhibited excellent cycling stability. While the specific capacity suffered an initial reduction, it then recovered to 100% (131 mAh g^{-1}) at 50th cycle and continued to increase to 148 mAh g^{-1} at 250th cycle with 100 mA g^{-1}. The detailed rate capacity of this sulfide polymer cathode has not been reported. In another report, poly(2,5-dihydroxyl-1,4-benzoquinonyl sulfide) (PDBS) was assessed as an organic cathode material in lithium ion battery. [90] The battery exhibits high initial discharge capacity of 350 mAh g^{-1} and reversible capacity of 250 mAh g^{-1} at 15 mA g^{-1}. It also shows good cycling stability (73.8% of the reversible capacity 184 mAh g^{-1} was retained at 100th cycle), good rate capacity (61.8% of capacity retained at 200 mA g^{-1} as compared to 15 mA g^{-1}) and high coulombic efficiency.

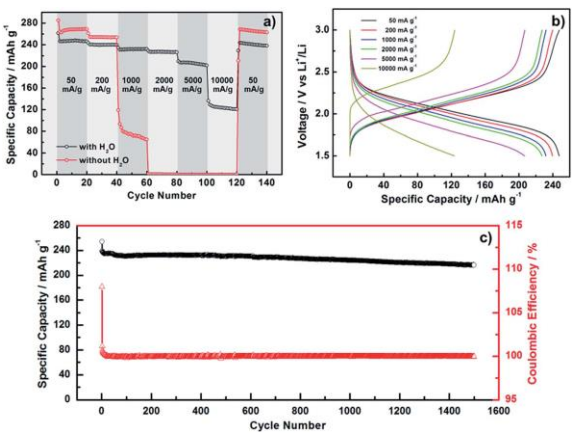

Scheme 11 (a) Discharge capacity profiles vs. cycle number of Li2PDHBQS electrodes with and without absorbed water, under sequentially changed current rate from 50 to 10000 mA g^{-1}. (b) Corresponding voltage profiles of Li2PDHBQS electrode with absorbed water, under different current rates. (c) Long-term cycling profiles of Li2PDHBQS electrode with absorbed water (1.5–3.0 V, 500 mA g^{-1}).[91]

More recently, Zhou's group further studied the PDBS polymer and its lithium salt ($Li_2PD(H)BS$) as organic cathode material in LIB.[91,92] The lithium salt of this sulfide polymer reduced its solubility drastically, rendering it completely insoluble in the electrolyte. The material demonstrated excellent cycling stability (90% capacity retention after 1500 cycles, 239 mAh g^{-1} at 500 mA g^{-1}), a dramatic improvement as compared to the parent PDBS polymer. Interestingly, it was reported that a small amount of water additive to the cathode material improves its rate capacity (Scheme 11), where a reversible capacity of 247 mAh g^{-1} at 50 mA g^{-1} was reported, with a capacity retention of Li_2PDHBS with H_2O is 94%, 83% and 50% at 1000, 5000 and 10000 mA g^{-1} respectively. In contrast, only 20% of the capacity (at 1000 mA g^{-1}) was retained for Li_2PDHBS without water. The outstanding performance of Li_2PDHBS cathode material was due to three aspects: the high charge/discharge rate of the quinone group, the presence of the Li ion and the presence of absorbed water in the cathode material that may help accelerate Li-ion transportation. The presence of water may partially dissolve Li_2PDHBS to promote the intimate contact of Ketjenblack carbon (conductive material) therefore improving its electronic conductivity. Irreversible side reactions were circumvented by strong hydrogen bonding between water and Li_2PDHBS, which prevents water from dissociating from the cathode to the electrolyte. Analogous Na_2PDHBS were also synthesized and exhibited similarly good performance in sodium ion battery.[93-95]

3.2.4 Conjugated linear polymers as organic electrode materials

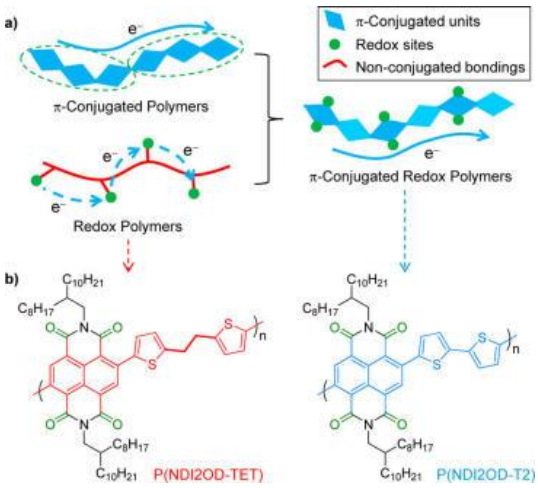

Scheme 12 (a) Graphical illustration of the structural characteristics of π-conjugated polymers, redox polymers, and π-conjugated redox polymers. (b) Molecular structure of the nonconjugated P(NDI2ODTET) and the π-conjugated P(NDI2OD-T2).[96]

Polyimide derivatives are well studied for its use as cathode materials in lithium or sodium ion battery.[43, 79-82] Typically, polyimides are synthesized by the reaction of aromatic ring bearing dianhydride moieties with diamines, and the resulting polymers exhibit improved cycling stabilities as compared to their parent monomeric materials. Examples of such dianhydrides include pyromellitic dianhydride (PMDA), 1,4,5,8-naphthalenetetracarboxylic dianhydride (NTCDA) and 3,4,9,10-perylenetetracarboxylic dianhydride (PTCDA). This type of nonconjugated redox polymers possess isolated redox active sites for accepting and releasing electrons. However, the efficiency of electron transport along the repeating units was very low. Recently, an n-dopable π-conjugated redox polymer was reported,[96] where the polymer was constructed by bridging naphthalene dicarboximide (NDI) derivatives with bithiophene (P(NDI2OD-T2) (Scheme 12). In this polymer, each NDI unit could reversibly accept two electrons, and will be delocalized in the repeating units of the polymer backbone, corresponding to an n-doping level of 2. As a comparison, a non-conjugated polymer with an ethylene linker between the bithiophene groups was synthesized (P(ZDI2OD-TET). While these two polymers have similar redox reaction rate and Li diffusivity rate, the electronic conductivity of bithiophene linked conjugated polymer is 4 orders higher than that of non-conjugated one. The intrachain charge transport within the π-conjugated backbone of P(NDI2OD-T2) dramatically increases the electronic conduction, resulting in an excellent rate capacity with 99% and 79% capacity retention at 10 C and 500 C respectively. In comparison, P(NDI2OD-TET) exhibits a capacity retention of 80% and 43% at 10 C and 500 C. However, the theoretical capacity of this polymer is low (54.2 mAh g^{-1}) due to the large molecule weight per unit.

In contrast, a non-conjugated polymer synthesized by condensation of pyromellitic dianhydride (PMDA) and 2,6-diaminoanthraquinone (AQ) (two different redox active sites, Scheme 13) exhibits high specific capacity of 190 mAh g^{-1} at 0.1 C and good cycling stability (91.5% capacity retention after 300 cycles).[97] Relatively good rate capacity of this polymer cathode (63% capacity retention at 20 C as compared to 0.1 C) was also

achieved after composition with highly conductive single-walled carbon nanotubes (SWNTs).

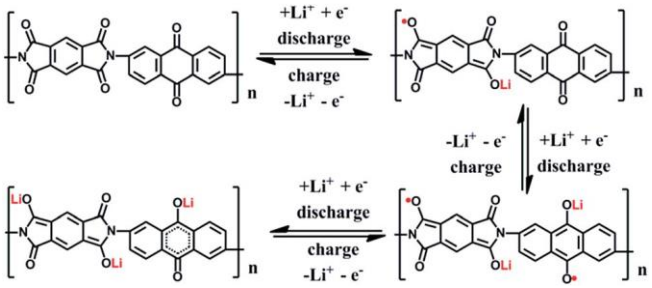

Scheme 13 Electrochemical redox reactions of PMAQ.[97]

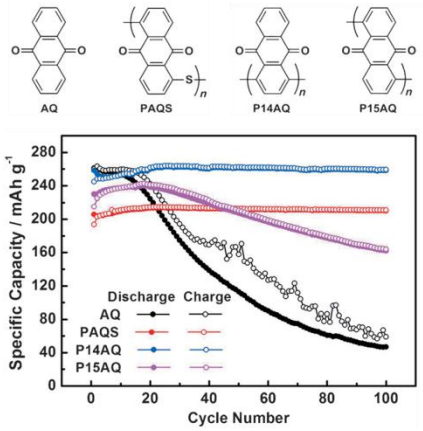

Scheme 14. Structure of AQ, PAQS, P14AQ, and P15AQ, and cycling profiles at a current rate of 0.2 C.[98]

Anthraquinone represents a class of well-studied organic cathode material and recent developments include the synthesis of polyanthraquinone via the direct crosslinking of the benzene rings, forming a conjugated structure to potentially achieve the maximum theoretical capacity.[98] Two regioisomeric-polymers were synthesized, where P14AQ and P15AQ refers to crosslinking at the 1,4 and 1,5 positions respectively (Scheme 14). Additionally a sulfur bridged polymer was also synthesized. As expected, P14AQ and P15AQ exhibit higher capacity than PAQS. P14AQ and PAQS also demonstrate excellent cycling stability with almost zero capacity decay after 100 cycles, and even 1000 cycles for P14AQ. Due to its low molecular weight (2300) and dissolution behaviour, P15AQ exhibits relatively poor cycling stability (67.6% capacity retention at 100th cycle). P14AQ also exhibits good rate capacity (69% capacity retention at 20 C as compared to the value at 0.2 C) which reflects its conjugated chain structure. In contrast, For P15AQ, the rate capacity is limited by the cycling stability.

In another report, π-conjugated polyazaacene analogue poly(1,6-dihydropyrazino[2,3g] quinoxaline-2,3,8-triyl-7-(*2H*)ylidene-7,8-dimethylidene) (PQL) was synthesized and applied as organic anode material for LIB.[99] This polymer anode material exhibits excellent initial capacity (1750 mAh g^{-1} at 0.05 C) and cycling stability (almost 100% capacity retention after 1000 cycles), but moderate rate capacity (17% capacity retention at 5 C as compared to 0.05 C). The moderate rate capacity could be due to the fact that the redox process breaks the π-conjugation system of the polymer backbone. More recently, a conjugated ladder polymer was developed as anode for LIB with high capacity and stable and fast cycling process.[100] Polymers based on Schiff bases have also been tested as electrode material for sodium ion battery.[101]

4. Two-dimensional organic networks toward improving kinetic parameters of LIB

There are several critical parameters which determine the kinetic performance of organic cathode materials: redox reaction rate, ion diffusion rate and electron transportation rate. The redox reaction rate is an intrinsic property of the redox active moiety and little improvements can be done by changing material morphologies. Attaching redox active sites within a porous organic framework could improve the ion diffusion rate, while embedding redox active sites within porous organic conjugated framework could enhance both ion diffusion rate and electronic conductivity.[102-103]

4.1 Non-conjugated porous COF materials

Theoretically, porous polymer materials are advantageous as organic cathode material due to their inherent insolubility and attractive porosity. However, the low processability of these two-dimensional polymers limits their practical applications. Efforts towards utilizing porous organic polymers in energy storage applications are more focused on increasing the capacity by forming electrochemical double-layers.[102,104] Recently, several examples of using porous organic polymers as organic cathode materials were reported. In particular, Jiang's group reported a crystalline, mesoporous, and redox active covalent organic framework (COF) cathode material.[105] This COF material (DTP-ANDI-COF) was constructed with a redox active naphthalene diimide (NDI), a triphenylene knot and boronate linkage (Scheme 15). This material has very high porosity and the electrode was prepared by directly growing the porous polymer on carbon nanotubes (CNT) which made up for the low electronic conductivity of non-conjugated DTP-ANDI-COF. In general, DTP-ANDI-COF@CNT cathode demonstrates excellent cycling stability with almost zero capacity decay after 700 cycles and fairly good rate capacity (85% capacity retention at 12 C as compared to 2.4 C). However, the specific capacity of this material is rather low (69 mAh g^{-1} at 2.4 C) due to the large molecular weight per redox active unit. In another report,[96] two porous COF materials were built by condensation of melamine with dianhydrides (pyromellitic dianhydride (PMDA-MEL) and naphthalene-1,4,5,8-tetracarboxylic dianhydride (NTCDA-MEL)). These two polyimide networks are used as anode material in sodium ion batteries where good cycling stability as well as moderate rate capacity was observed.

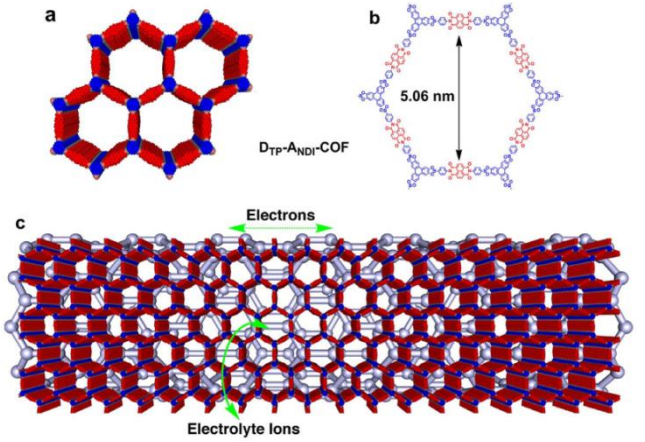

Scheme 15 Structure of redox-active organic electrode materials. (a and b), Structures of DTP-ANDI-COF. (c), Graphical representation of DTP-ANDI-COF@CNTs (grey for CNTs) and electron conduction and ion transport.[105]

4.2 Conjugated porous organic frameworks

Conjugated microporous polymers (CMPs) have been well studied as energy storage materials.[102, 107-115] The first instance of CMPS utilized as organic cathode materials for lithium batteries was recently reported by Jiang's group.[116] This hexaazatrinaphthalene CMP (HATN-CMP) has high porosity, rigid 2D structure and extended conjugation framework (Scheme 16). HATN-CMP exhibits a discharge capacity of 147 mAh g^{-1} at 100 mA g^{-1} with 71% of theoretical capacity. However, HATN-CMP unexpectedly exhibits relatively poor cycling stability with 62% capacity retention after 50 cycles. The rate capacity of this CMP cathode was also relatively poor, with 44% capacity retention at 500 mA g^{-1} as compared to the capacity at 100 mA g^{-1}. Though these conjugated porous polymers possess high porosity and high electronic conductivity, which are proposed to have positive influence on the kinetic parameters of LIB, the poor cycling stability and rate capacity may due to the poor redox stability of the highly conjugated redox system. In another report, a conjugated polymer 4,7-dicarbazyl-[2,1,3]-benzothiadiazole (PDCzBT) was developed as organic cathode material for lithium ion and sodium ion batteries (Scheme 17).[117] PDCzBT has excellent porosity (surface area 1162 m^2 g^{-1}), its conjugation system was much more limited in one dimension as compared to HATN-CMP. However, PDCzBT electrode exhibits excellent cycling capacity (no capacity decay after 400 cycles), but moderate rate capacity was observed (about 40% capacity retention at 2000 mA g^{-1} as compared to the value at 200 mA g^{-1}). The excellent cycling stability could be attributed to the stable and insoluble network structure and the stable and reversible redox reaction, with the homogeneous microporeous structure advantageous Li ion diffusion. The one-dimension conjugation system of the polymer makes it a relatively good electronic conductor. However, considering the morphology of bulky polymer material and the long electron transportation distance within the electrode, electronic conductivity is still the main factor which limits the rate capacity of PDCzBT electrode.

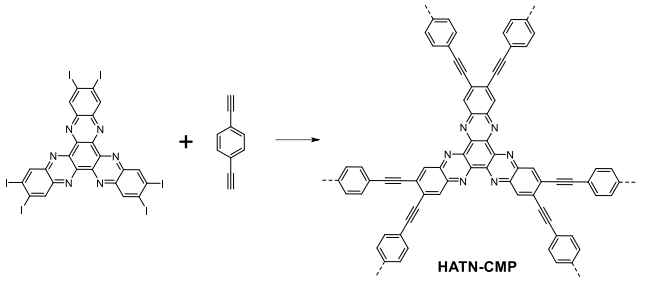

Scheme 16 Schematic representation of the synthesis of hexaazatrinaphthalene CMP (HATN-CMP).[116]

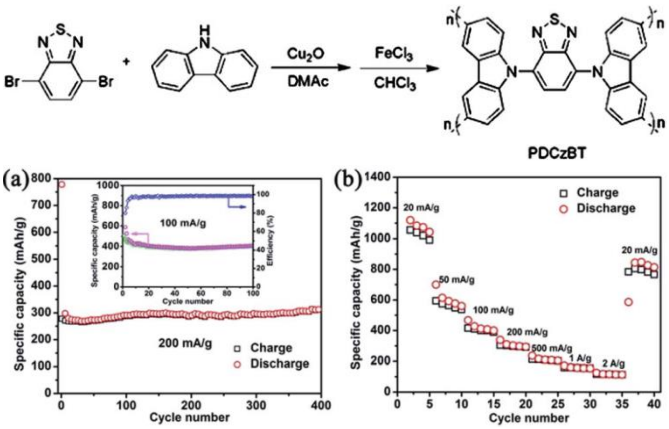

Scheme 17 Synthetic route of conjugated microporous polymer PDCzBT and Electrochemical performance of the PDCzBT electrode for LIBs. (a) Cycle performance at a current density of 200 mA g^{-1}. Inset: cycle performance and coulombic efficiency at 100 mA g^{-1}; (b) Rate performance at varied current density ranging from 20 to 2000 mA g^{-1}.[117]

4.3 Polymer-Graphene nanocomposites

The major limitations that prevent the application of organic electrode materials in lithium ion batteries are their high solubility in the electrolyte and low conductivity. While a polymeric organo-electrode solves the dissolution limitation, most systems are plagued by low conductivities, especially for bulky and rigid 2 or 3-dimensional frameworks. The poor processability and large particle size weaken the contact between redox active materials and conductive materials, and therefore consequently increase the electron transportation distance. However, a strategy of synthesizing a composite consisting of redox active sites and a conductive material may solve these issues. In this particular design, the redox active molecule is directly linked to the surface of conductive material (such as graphene) or polymerized on the surface of graphene in situ. The organic redox materials are then homogeneously coated on the surface of conductive material with close and/or direct contact. To this end, there has been much effort devoted on electrode structure design in battery studies.[118-120]

Wang et al. reported polymer-graphene nanocomposite cathode materials by directly synthesizing poly(anthraquinonyl sulfide) (PAQS) or polyimide (PI) on the surface of functionalized graphene sheets (FGSs).[121] The polymers are homogeneously deposited on the

graphene with noncovalent interaction (Scheme 18), and the resultant surface area and electronic conductivity of the nanocomposite materials were dramatically improved. The nanocomposite electrode (PAQS-FGS (26 wt%)) exhibits excellent cycling stability and rate capacity (90% of capacity retention at 10 C as compared to the value at 0.1 C). The cycling stability and rate capacity of PI-FGS also demonstrate evident improvement in comparison with PI cathode. More recently, Feng's group reported a graphene-porous polyaryltriazine nanocomposite cathode for lithium ion battery and remarkable electrochemical performance was observed.[122] Bi-polar porous triazine framework has also been studied as organic cathode material in LIB.[123] Here, the material was synthesized by polymerizing dicyanobenzene on polyacrylonitrile-functionalized graphene (G-PPF) at temperature between 400 °C to 600 °C in $ZnCl_2$. In this material, the triazine framework is homogeneously attached to the graphene through covalent bonding. This nanocomposite cathode exhibits super high capacity, high cycling stability and high rate capacity (Scheme 19). The best sample (G-PPF-p-400-600) delivers a reversible capacity of 395 mAh g^{-1} at 5 A g^{-1} even after 5100 cycles. During 5000 cycles at 5 A g^{-1}, the increase in capacity was slow but eventually stabilized at 395 mAh g^{-1}. This is a remarkable result for organic cathode materials in lithium ion batteries. The excellent performance of this material could be attributed to its nanocomposite structure where porous triazine network is covalently bound to graphene sheet. This nanocomposite material is insoluble, has porous structure for good ion diffusion and also has excellent electronic conductivity. However, the material synthesis is rather complex and may not be suitable for large scale production.

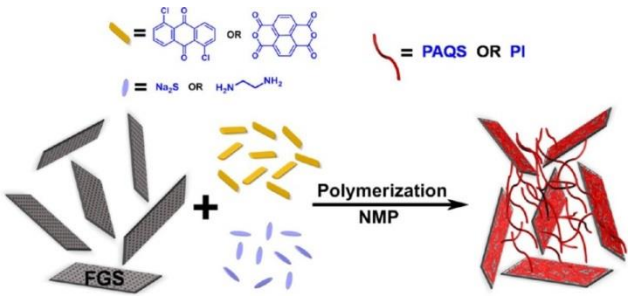

Scheme 18 In situ polymerization process of PAQS-FGS or PI-FGS nanocomposite.[121]

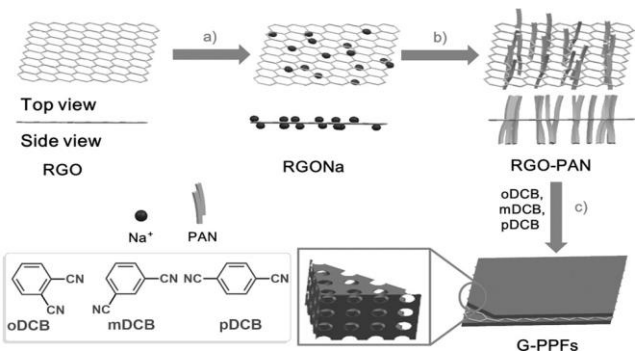

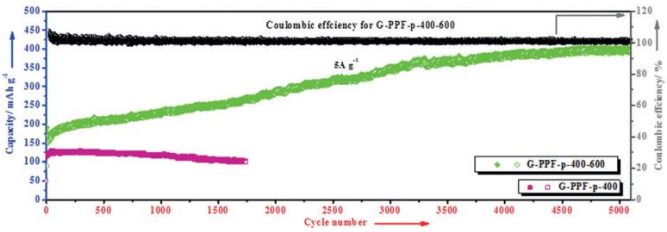

Scheme 19 Compact coupled graphene and porous polyaryltriazine derived frameworks. a) The formation of graphene-based 2D carbanions. b) Anionic polymerization of acrylonitrile on the surface of RGO. c) The trimerization of dicyanobenzene. Bottom: Cycle performance of G-PPF-p-400-600 electrode (up to 5100 cycles) and G-PPF-p-400 electrode (up to 1600 cycles) at a current density of 5.0 A g^{-1}.[122]

5. Conclusions and outlook

Although the industrial application of organic electrode materials in lithium ion battery still needs to be proven, laboratory development of organic electrode materials has demonstrated interesting potential. As an example, the related energy density of G-PPF-p-400-600 electrode (scheme 19) is 1185 Wh/Kg, which is much higher than typical current inorganic cathode materials (about 200 Wh/Kg). Organic materials are green and more sustainable. However, these materials have their intrinsic drawbacks including solubility in electrolyte media, variable redox stability and low electronic conductivity. Various approaches have been investigated to improve the performance of organic electrodes in lithium (sodium) ion batteries. However, most of these approaches work towards improving one or two parameters of electrode materials, which will limit the overall performance of the battery. Modifying the backbone structure of the redox active moiety may improve its redox potential, redox stability and reaction rates related to the specific capacity and rate capacity of battery. In comparison, the polymerization of redox active molecule may help reduce its solubility, and increase ion diffusion and electronic conductivity, specific factors that are related to cycling stability, rate capacity and also specific capacity of battery. However, it is very challenging to introduce improvements in all the mentioned parameters in one structure. It is crucial to balance all parameters related to electrode material to achieve optimal overall performance. To this point, understanding the properties of various new materials and their consequent effect on all electrode parameters is important. Such studies will also guide the development of new organic electrode materials. The development of new, effective organic electrode materials has seen much promising growth where recent strategies of polymerization of small organic redox active molecules, embedding them into porous organic frameworks and the synthesis of organic-inorganic composites are indeed moves in the right direction. In addition, electrolyte is another important parameter for electrochemical performance of electrode materials.[124] The study of the interaction between electrolyte and electrode should be enhanced. Further research efforts should be devoted on new strategies that can balance and optimize parameters to improve the utility of the electrode material.

Acknowledgements

This work was supported by the Institute of Bioengineering and Nanotechnology (Biomedical Research Council, Agency for Science, Technology and Research (A*STAR), Singapore).

References

1 N. S. Choi, Z. Chen, S. A. Freunberger, X. Ji, Y. K. Sun, K. Amine, G. Yushin, L. F. Nazar, J. Cho and P. G. Bruce, *Angew. Chem. Int. Ed.,* 2012, **51**, 9994-10024.
2 J. B. Goodenough and K. S. Park, *J. Am. Chem. Soc.,* 2013, **135**, 1167-1176.
3 K. Zhang, X. Han, Z. Hu, X. Zhang, Z. Tao and J. Chen, *Chem. Soc. Rev.,* 2015, **44**, 699-728.
4 Y. Tang, Y. Zhang, W. Li, B. Ma and X. Chen, *Chem. Soc. Rev.,* 2015, **44**, 5926-5940.
5 D. W. Wang, Q. Zeng, G. Zhou, L. Yin, F. Li, H. Chen, I. R. Gentle and G. Lu, *J. Mater. Chem. A.,* 2013, **1**, 9382-9394.
6 M. Barghamadi, A. S. Best, A. I. Bhatt, A. F. Hollenkamp, M. Musameh, R. J. Rees and T. Ruther, *Energy Environ. Sci.,* 2014, **7**, 3902-3920.
7 J. Chen and F. Cheng, *Acc. Chem. Res.,* 2009, **42**, 713-723.
8 A. K. Padhi, K. S. Nanjundaswamy and J. B. Goodenough, *J. Electrochem. Soc.,* 1997, **144**, 1188-1194.
9 M. S. Whittingham, *Chem. Rev.,* 2014, **114**, 11414-11443.
10 10. D. L. Williams, J. J. Byrne and J. S. Driscoll, *J. Electrochem. Soc.,* 1969, **116**, 2-4.
11 Y. Liang, Z. Tao and J. Chen, *Adv. Energy Mater.,* 2012, **2**, 742-769.
12 G. Milcarek and O. Inganas, *Science*, 2012, **335**, 1468-1471.
13 Z. Song and H. Zhou, *Energy Environ. Sci.,* 2013, **6**, 2280-2301.
14 X. Han, G. Qing, J. Sun and T. Sun, *Angew. Chem. Int. Ed.,* 2012, **51**, 5147-5151.
15 M. Lee, J. Hong, D. H. Seo, D. H. Nam, K. T. Nam, K. Kang and C. B. Park, *Angew. Chem. Int. Ed.,* 2013, **52**, 8322-8228.
16 J. Hong, M. Lee, B. Lee, D. H. Seo, C. B. Park and K. Kang, *Nat. Comm.,* 2014, **5**, 5335-5344.
17 P. J. Nigrey, D. Maclnnes, D. P. Nairns and A. G. MacDiarmid, *J. Electrochem. Soc.,* 1981, **128**, 1651-1654.
18 L. W. Shacklette, J. E. Toth, N. S. Murthy and R. H. Baughman *J. Electrochem. Soc.,* 1985, **132**, 1529-1535.
19 N. Mermilliod, J. Tanguy and F. Petiot, *J. Electrochem. Soc.,* 1986, **133**, 1073-1079.
20 N. Gospodinova and L. Terlemezyan, *Prog. Polym. Sci.,* 1998, **23**, 1443-1484.
21 M. Zhou, J. Qian, X. Ai and H. Yang, *Adv. Mater.,* 2011, **23**, 4913-4917.
22 K. Nakahara and S. Iwasa, M. Satoh, Y. Morioka, J. Iriyama M. Suguro and E. Hasegawa, *Chem. Phys. Lett.,* 2002, **359**, 351-564.
23 H. Nishide and S. Iwasa, Y. J. Pu, T. Suga, K. Nakahara and M. Satoh, *Electrochim. Acta,* 2004, **50**, 827-831.
24 T. Suga and H. Konishi and H. Nishide, *Chem. Commun.,* 2007, **17**, 1730-1732.
25 K. Oyaizu, T. Suga, K. Yoshimura and H. Nishide, *Macromolecules,* 2008, **41**, 6646-6652.
26 W. Choi, S. Ohtani, K. Oyaizu, H. Nishide and K. E. Geckeler, *Adv. Mater.,* 2011, **23**, 4440-4443.
27 S. J. Visco and L. C.De Jonghe, *J. Electrochem. Soc.,* 1988, **135**, 2905-3176.
28 M. Liu, S. J., Visco and L. C. De Jonghe, *J. Electrochem. Soc.,* 1990, **137**, 750-759.
29 N. Oyama, T. Tatsuma, T. Sato and T. Sotomura, *Nature,* 1995, 373, 598-600.
30 K. Naoi, K. I. Kawase, M. Mori and M. Komiyama M, *J. Electrochem. Soc.,* 1997, **144**, L173-L175.
31 N. Oyama, J. M. Pope and T. Sotomura T, *J. Electrochem. Soc.,* 1997, **144**, L47-L51.
32 S. I. Tobishima and J. I. Yamaki and A. Yamaji, *J. Electrochem. Soc.,* 1984, **131**, 57-63.
33 J. S. Foos, S. M. Erker and L. M. Rembetsy, *J. Electrochem. Soc.,* 1986, **133**, 836-841.
34 D. Häringer, P. Novák, O. Haas, B. Piro and M. C. Pham, *J. Electrochem. Soc.*, 1999, **146**, 2393-2396.
35 L. Fedele, F. Sauvage, J. Bois, J. M. Tarascon and M. Becuwe, *J. Electrochem. Soc.,* 2014, **161**, A46-A52.
36 K. Sakaushi and M. Antonietti, *Acc. Chem. Res.,* 2015, **48**, 1591-1600.
37 T. Matsunaga, T. Kubota, T. Sugimoto and M. Satoh, *Chem. Lett.,* 2011, **40**, 750-752.
38 Y. Liang, P. Zhang and J. Chen, *Chem. Sci.,* 2013, **4**, 1330-1337.
39 H. G. Wang, S. Yuan, Z. Si and X. B. Zhang, *Energy Environ. Sci.,* 2015, **8**, 3160-3165.
40 C. Su, X. Zhu, L. Xu, N. Zhou, H. He and C. Zhang, *Electrochimica Acta,* 2016, **196**, 440-449.
41 H. Chen, M. Armand, G. Demailly, F. Dolhem, P. Poizot and J. M. Tarascon, *ChemSusChem,* 2008, **1**, 348.
42 X. Han, C. Chang, L. Yuan, T. Sun and J. Sun, *Adv. Mater.,* 2007, **19**, 1616-1621.
43 Z. Song, H. Zhan and Y. Zhou, *Angew. Chem. Int. Ed.,* 2010, **49**, 8444-8448.
44 M. Armand, S. Grugeon, H. Vezin, S. Laruelle, P. Ribiere, P. Poizot and J. M. Tarascon, *Nat. Mater.,* 2009, **8**, 120-125.
45 H. Chen, M. Armand, M. Courty, M. Jiang, C. P. Grey, F. Dolhem, J. M. Tarascon and P. Poizot, *J. Am. Chem. Soc.,* 2009, **131**, 8984-8988.
46 S. Wang, L. Wang, K. Zhang, Z. Zhu, Z. Tao and J. Chen, *Nano Lett.,* 2013, **13**, 4404-4409.
47 C. Luo, R. Huang, R. Kevorkyants, M. Pavanello, H. He and C. Wang, *Nano Lett.,* 2014, **14**, 1596-1602.
48 Y. Hanyu and I. Honma, *Sci. Rep.,* 2012, **2**, 453-459.
49 Y. Hanyu, Y. Ganbe and I. Honma, *J. Power Sources,* 2013, **221**, 186-190.
50 Z. Zhu, M. Hong, D. Guo, J. Shi, Z. Tao and J. Chen, *J. Am. Chem. Soc.,* 2014, **136**, 16461-16466.
51 B. Genorio, K. Pirnat, R. Cerc-Korosec, R. Dominko and M. Gaberscek, *Angew. Chem. Int. Ed.,* 2010, **49**, 7222-7224.
52 K. Pirnat, R. Dominko, R. Cerc-Korosec, G. Mali, B. Genorio and M. Gaberscek, *J. Power Sources,* 2012, **199**, 308-314.
53 P. Poizot and F. Dolhem, *Energy Environ. Sci.,* 2011, **4**, 2003-2019.
54 Z. Zhu and J. Chen, *J. Electrochem. Soc.,* 2015, **162**, A2393-A2405.
55 P. Novák, K. Müller, K. S. V. Santhanam and O. Haas, *Chem. Rev.,* 1997, **97**, 207-282.
56 T. Janoschka, M. D. Hager and U. S. Schubert, *Adv. Mater.,* 2012, **24**, 6397-6409.
57 R. Gracia and D. Mecerreyes, *Polym. Chem.,* 2013, **4**, 2206-2214.
58 B. Häupler, A. Wild and U. S. Schubert, *Adv. Energy Mater.,* 2015, **5**, 1402034-1402068.
59 F. Vilela, K. Zhang and M. Antonietti, *Energy Environ. Sci.,* 2012, **5**, 7819-7832.
60 T. B. Schon, B. T. McAllister, P.-F. Li and D. S. Seferos, *Chem. Soc. Rev.*, 2016, DOI:10.1039/c6cs00173d
61 J. Xie and Q. Zhang, *J. Mater. Chem. A*, 2016, **4**, 7091-7106.
62 Y. Morita, S. Nishida, T. Murata, M. Moriguchi, A. Ueda, M. Satoh, K. Arifuku, K. Sato and T. Takui, *Nat. Mater.,* 2011, **10**, 947-951.
63 C. Wang, Y. Xu, Y. Fang, M. Zhou, L. Liang, S. Singh, H. Zhao, A. Schober and Y. Lei, *J. Am. Chem. Soc.,* 2015, **137**, 3124-3130.
64 A. Kuhn, K. G. von Eschwege and J. Conradie, *J. Phys. Org. Chem.,* 2012, **25**, 58-68.

65 M. Park, D.-S. Shin, J. Ryu, M. Choi, N. Park, S. Y. Hong and J. Cho, *Adv. Mater.,* 2015, **27**, 5141-5146.
66 G. S. Vadehr, R. P. Maloney, M. A. Garcia-Garibay and B. Dunn, *Chem. Mater.,* 2014, **26**, 7151-7157.
67 K. Hernandez-Burgos, S. E. Burkhardt, G. G. Rodriguez-Calero, R. G. Hennig and H. D. Abruna, *J. Phys. Chem. C*., 2014, **118**, 6046-6051.
68 E. Clar, Polycyclic Hydrocarbons, Academic Press, New York, 1964.
69 D. Wu, Z. Xie, Z. Zhou, P. Shen and Z. Chen, *J. Mater. Chem. A.,* 2015, **3**, 19137-19143.
70 M. E. Bhosale and K. Krishnamoothy, *Chem. Mater.,* 2015, **27**, 2121-2126.
71 Z. Q. Zhu, M. L. Hong, D. S. Guo, J. F. Shi, Z. L. Tao and J. Chen, *J. Am. Chem. Soc.,* 2014, **136**, 16461-16464.
72 D. Chen, A.-J. Avestro, Z. Chen, J. Sun, S. Wang, M. Xiao, Z. Erno, M. M. Algaradah, M. S. Nassar, K. Amine, Y. Meng and J. F. Stoddart, *Adv. Mater.,* 2015, **27**, 2907-2912.
73 S. T. Schneebeli, M. Frasconi, Z. Liu, Y. Wu, D. M. Gardner, N. L. Strutt, C. Cheng, R. Carmieli, M. R. Wasielewski and J. F. Stoddart, *Angew. Chem. Int. Ed.,* 2013, **52**, 13100-13104.
74 A. Shimizu, H. Kuramoto, Y. Tsujii, T. Nokami, Y. Inatomi, N. Hojo, H. Suzuki and J.-I. Yoshida, *J. Power Sources,* 2014, **260**, 211-217.
75 M. Lv, F. Zhang, Y. Wu, M. Chen, C. Yao, J. Nan, D. Shu, R. Zeng, H. Zeng and S.-L. Chou, *Sci. Rep.,* 2016, **6**, 23515-23522.
76 S. R. Forrest, *Chem. Rev.* 1997, **97**, 1793-1896.
77 A. Abouimrane, W. Weng, H. Eltayeb, Y. Cui, J. Niklas, O. Poluektov and K. Amine, *Energy Environ. Sci*., 2012, **5**, 9632-9638.
78 Y. F. Shen, D. D. Yuan, X. P. Ai, H. X. Yang and M. Zhou*, J. Polymer Sci., B,* 2015, **53**, 235-238.
79 H. Banda, D. Damien, K. Nagarajan, M. Hariharan and M. M. Shaijumon, *J. Mater. Chem. A.,* 2015, **3**, 10453-10458.
80 T. Le Gall, K. H. Reiman, M. C. Grossel and J. R. Owen, *J. Power Sources,* 2003, **119-121**, 316-320.
81 H. Wu, S. A. Shevlin, Q. Meng, W. Guo, Y. Meng, K. Lu, Z. Wei and Z. Guo, *Adv. Mater.,* 2014, **26**, 3338-3343.
82 G. Hernandez, N. Casado, R. Coste, D. Shanmukaraj, L. Rubatat, M. Armand and D. Mecerreyes, *RSC Adv.,* 2015, **5**, 17096-17103.
83 P. Sharma, D. Damien, K. Nagarajan, M. M. Shaijumon and M. Hariharan, *J. Phys. Chem. Lett.,* 2013, **4**, 3192-3197.
84 T. Nokami, T. Matsuo, Y. Inatomi, N. Hojo, T. Tsukagoshi, H. Yoshizawa, A. Shimizu, H. Kuramoto, K. Komae, H. Tsuyama and J.-I. Yoshida, *J. Am. Chem. Soc.,* 2012, **134**, 19694-19700.
85 B. Haupler, T. Hagemann, C. Friebe, A. Wild and U. S. Schubert, *ACS Appl. Mater. Interfaces* 2015, **7**, 3473-3481.
86 Z. Song, T. Xu, M. L. Gordin, Y. B. Jiang, I. T. Bae, Q. Xiao, H. Zhan, J. Liu and D. Wang, *Nano Lett*., 2012, **12**, 2205–2211.
87 W. Xu, A. Read, P. K. Koech, D. Hu, C. Wang, J. Xiao, A. B. Padmaperuma, G. L. Graff, J. Liu and J.-G. Zhang, *J. Mater. Chem.*, 2012, **22**, 4032.
88 T. Ma, Q. Zhao, J. Wang, Z. Pan and J. Chen, *Angew. Chem. Int. Ed.*, 2016, **55**, 6428-6432.
89 X. Han, C. Chang, L. Yuan, T. Sun and J. Sun, *Adv. Mater.,* 2007, 19, 1616.
90 K. Liu, J. Zheng, G. Zhong and Y. Yang, *J. Mater. Chem.,* 2011, **21**, 4125-4131.
91 Z. Song, Y. Qian, X. Liu, T. Zhang, Y. Zhu, H. Yu, M. Otani and H. Zhou, *Energy Environ. Sci.,* 2014, **7**, 4077-4086.
92 Z. Song, Y. Qian, T. Zhang, M. Otani and H. Zhou, *Adv. Sci*., 2015, **2**, 1500124.
93 S. Wang, L. Wang, Z. Zhu, Z. Hu, Q. Zhao and J. Chen, *Angew. Chem. Int. Ed.,* 2014, **53**, 5892-5896.
94 H. G. Wang, S. Yuan, D.-I. Ma, X.-I. Huang, F.-I. Meng and X.-B. Zhang, *Adv. Energy Mater.,* 2014, **4**, 1301651-1301658.
95 W. Deng, X. Liang, X. Wu, J. Qian, Y. Cao, X. Ai, J. Feng and H. Yang, *Sci. Rep*., 2013, **3**, 2671.
96 Y. Liang, Z. Chen, Y. Jiang, Y. Rong, A. Facchetti and Y. Yao, *J. Am. Chem. Soc.,* 2015, **137**, 4956-4959.
97 H. P. Wu, Q. Yang, Q. H. Meng, A. Ahmad, M. Zhang, L. Y. Zhu, Y. G. Liu and Z. X. Wei, *J. Mater. Chem., A* 2016, 4, 2115-2121.
98 Z. Song, Y. Qian, M. L. Gordin, D. Tang, T. Xu, M. Otani, H. Zhang, H. Zhou and D. Wang, *Angew. Chem. Int. Ed*., 2015, **54**, 13947-13951.
99 J. Wu, X. Rui, G. Long, W. Chen, Q. Yan and Q. Zhang, *Angew. Chem. Int. Ed.,* 2015, **54**, 7354-7358.
100 J. Wu, X. Rui, C. Wang, W.-B. Pei, R. Lau, Q. Yan and Q. Zhang, *Adv. Energy Mater*., 2015, **6**, 1402189.
101 E. Castillo-Martinez, J. Carretero-Gonzalez and M. Armand, *Angew. Chem. Int. Ed.,* 2014, **53**, 5341-5345.
102 Y. Shi, L. Peng, Y. Ding, Y. Zhao and G. Yu, *Chem. Soc. Rev.,* 2015, **44**, 6684-6696.
103 S. N. Talapaneni, T. H. Hwang, S. H. Je, O. Buyukcakir, J. W. Choi and A. Coskun, *Angew. Chem. Int. Ed.,* 2016, **55**, 3106-3111.
104 C. R. DeBlase, K. Hernandez-Burgos, J. M. Rotter, D. J. Fortman, D. dos S. Abreu, R. A. Timm, I. C. N. Diogenes, L. T. Kubota, H. D. Abruna and W. R. Dichtel, *Angew. Chem. Int. Ed.,* 2015, **54**, 13225-13229.
105 F. Xu, S. Jin, H. Zhong, D. Wu, X. Yang, X. Chen, H. Wei, R. Fu and D. Jiang, *Sci. Rep.,* 2015, **5**, 8225-8231.
106 Z. Li, J. Zhou, R. Xu, S. Liu, Y. Wang, P. Li, W. Wu and M. Wu, *Chem. Engineer. J.,* 2016, **287**, 516-552.
107 Y. Kou, Y. Xu, Z. Guo and D. Jiang, *Angew. Chem. Int. Ed.,* 2011, **50**, 8753-8757.
108 M. E. Bhosale, R. Illathvalappil, S. Kurungot and K. Krishnamoorthy, *Chem. Commun.,* 2016, **52**, 316-318.
109 P. Wang, Q. Wu, L. Han, S. Wang, S. Fang, Z. Zhang and S. Sun, *RSC Adv.,* 2015, **5**, 27290-27294.
110 K. Sakaushi, E. Hosono, G. Nickerl, T. Gemming, H. Zhou, S. Kaskel and J. Eckert, *Nat. Comm.,* 2013, **4**, 1485-1497.
111 H. Ding, Y. Li, H. Hu, Y. Sun, J. Wang, C. Wang, C. Wang, G. Zhang, B. Wang, W. Xu and D. Zhang, *Chem. Eur. J.,* 2014, **20**, 14614-14618.
112 Z. Xiang, D. Cao and L. Dai, *Polym. Chem.,* 2015, **6**, 1896–1911;
113 J.-J. Adjizian, A. Lherbier, S. M.-M. Dubois, A. R. Botello-Méndez and J.-C. Charlier, *Nanoscale,* 2016, **8**, 1642-1651.
114 Y. Xu, S. Jin, H. Xu, A. Nagai and D. Jiang, *Chem. Soc. Rev.,* 2013, **42**, 8012-8031.
115 X.-H. Liu, C.-Z. Guan, D. Wang and L.-J. Wan, *Adv. Mater.,* 2014, **26**, 6912–6920.
116 F. Xu, X. Chen, Z. Tang, D. Wu, R. Fu and D. Jiang, *Chem. Commun.,* 2014, **50**, 4788-4790.
117 S. Zhang, W. Huang, P. Hu, C. Huang, C. Shang, C. Zhang, R. Yang and G. Cui, *J. Mater. Chem. A*., 2015, **3**, 1896-1901.
118 B. Jeong, J. D. Ocon and J. Lee, *Angew. Chem. Int. Ed.*, 2016, **55**, 4870-4880.
119 S. W. Lee, N. Yabuuchi, B. M. Gallant, S. Chen, B.-S. Kim, P. T. Hammond and Y. Shao-Horn, *Nat. Nanotech.,* 2010, **5**, 531-537.
120 X. Zhuang, D. Gehrig, N. Forler, H. Liang, M. Wagner, M. R. Hansen, F. Laquai, F. Zhang, and X. Feng, *Adv. Mater.,* 2015, **27**, 3789-3796.
121 Z. Song, T. Xu, M. L. Gordin, Y.-B. Jiang, I.-T. Bae, Q. Xiao, H. Zhan, J. Liu and D. Wang, *Nano Lett.,* 2012, **12**, 2205-2221.
122 Y. Su, Y. Liu, P. Liu, D. Wu, X. Zhuang, F. Zhang and X. Feng, *Angew Chem. Int. Ed.,* 2015, **54**, 1812-1816.
123 K. Sakaushi, G. Nickerl, F. M. Wisser, D. Nishio-Hamane, E. Hosono, H. Zhou, S. Kaskel and J. Eckert, *Angew. Chem. Int. Ed.*, 2012, **51**, 7850-7854.

124 M. R. Busche, T. Drossel, T. Leichtweiss, D. A. Weber, M. Falk, M. Schneider, M.-L. Reich, H. Sommer, P. Adelhelm, J. Janek, *Nat. Chem.*, DOI: 10.1038/NCHEM.2470

TOC